Estimating geometrical and mechanical REV based on synthetic rock mass models at Brunswick Mine

Kamran Esmaieli[1], John Hadjigeorgiou[1], and Martin Grenon[2]

[1]*Lassonde Institute, University of Toronto, Toronto, Canada*

[2]*Faculté des sciences et de génie, Département de génie des mines, de la métallurgie et des matériaux, Université Laval, Québec, Canada*

ABSTRACT

This paper uses a case study from Brunswick Mine in Canada to determine a representative elementary volume (REV) of a jointed rock mass in the vicinity of important underground infrastructure. The equivalent geometrical and mechanical property REV sizes were determined based on fracture systems modeling and numerical experiments on a synthetic rock mass. Structural data collected in massive sulphides were used to generate a large fracture system model (FSM), 40 m x 40 m x 40 m. This FSM was validated and subsequently sampled to procure 40 cubic specimens with a height to width ratio of 2 based on sample width from 0.05 to 10 m. The specimens were introduced into a 3D particle flow code (PFC3D) model to create synthetic rock mass (SRM) samples. The geometrical REV of the rock mass was determined based on the number of fractures in each sampled volume (P_{30}) and the volumetric fracture intensity (P_{32}) of the samples. The mechanical REV was estimated based on the uniaxial compressive strength (UCS) and elastic modulus (E) of the synthetic rock mass samples. The REV size of the rock mass was determined based on a series of statistical tests. The T-test was used to assess whether the means of the samples were statistically different from each other and the F-test to compare the calculated variance. Finally, the coefficient of variation, for the synthetic rock mass geometrical and mechanical properties, was plotted against sample size. For this particular site the estimated geometrical REV size of the rock mass was 3.5 m x 3.5 m x 7 m, while the mechanical property REV size was 7 m x 7 m x 14 m. Consequently, for engineering purposes the largest volume (7 m x 7 m x 14 m) can be considered as the REV size for this rock mass.

KEYWORDS

Underground mining, Representative elementary volume (REV), Fracture system model, Synthetic rock mass, Mechanical properties, Distinct modeling

CITATION

Esmaieli K, Hadjigeorgiou J, & Grenon M. Estimating geometrical and mechanical REV based on synthetic rock mass models at Brunswick Mine. International Journal of Rock Mechanics and Mining Sciences (2010) 47(6), 915-926.

This is the author's version of the original manuscript. The final publication is available at Elsevier Link Online via doi:10.1016/j.ijrmms.2010.05.010

1 INTRODUCTION

A jointed rock mass is defined by the presence of fracture defects. These can be large scale geological structures, such as faults and dykes which can extend to tens or hundreds of meters or medium scale fractures, such as joints, bedding planes and foliations which can be anywhere from

a few centimeters to tens of meters. For engineering purposes a critical design parameter is the relative size of geological fractures with respect to excavation size.

Determining the mechanical properties of intact rock samples in the laboratory is relatively straightforward. The challenge is to extrapolate from standard laboratory tests to predict the field behavior of rock masses. A common engineering assumption is that the mechanical properties of jointed rock are lower than that of intact rock. In well defined and connected rock fractures, the mechanical behavior of a jointed rock mass is controlled by the fracture characteristics. In cases, however, where fractures do not intersect to form well defined blocks, the behavior of a rock mass is also influenced by the strength of intact rock bridges between fractures.

Krauland et al. [1] distinguish four strategies applicable to the determination of mechanical properties of a rock mass: mathematical models, rock mass classification, large scale testing and back-analysis of failures. Mathematical models often simulate intact rock and fractures as discrete elements in the rock mass. They rely on simplifying assumptions and frequently require the determination of a large number of parameters. Classification methods, on the other hand, use selected rock mass properties to determine a representative index of rock mass quality. This index is often linked to rock mass failure criteria that can be used to predict the behavior of a rock mass. Rock mass classification techniques are popular even though the assumption that a unique index can capture the behavior of a structurally complex rock mass is debatable. The relevant mechanical properties of a rock mass can also be determined by using large in situ tests. Such tests are quite difficult to undertake and can be very expensive and difficult to justify. The use of large scale laboratory tests is limited by sampling considerations and the inherent difficulties of manipulating large rock mass samples. An interesting approach for the determination of the mechanical properties of a rock mass is the use of back-analysis of reported failures. This, however, requires that the failure mechanism is well defined and understood which is not always the case in complex geological environments.

The scale dependency of rock mass behavior is well documented [1–4]. One way to quantify this scale dependency is by using the representative elementary volume (REV) of a rock mass as illustrated in Fig. 1, after Hudson and Harrison [5]. REV is the volume at which the size of the tested sample contains a sufficient number of inhomogeneities for the ‘‘average value’’ to be reasonably consistent under repeated testing. The REV can be used to determine whether a rock mass can appropriately be treated as an equivalent continuum. This has important implications in the choice of numerical analysis tools. Furthermore, when the rock mass volume is equal or bigger than the REV, it is justifiable to use an average value for the rock mass property of interest. It follows that different mechanical, hydraulic, thermal, geometrical or any other rock mass properties can have a different REV. In addition, in an anisotropic rock mass, REV size for certain properties such as fracture spacing is also influenced by sampling orientation.

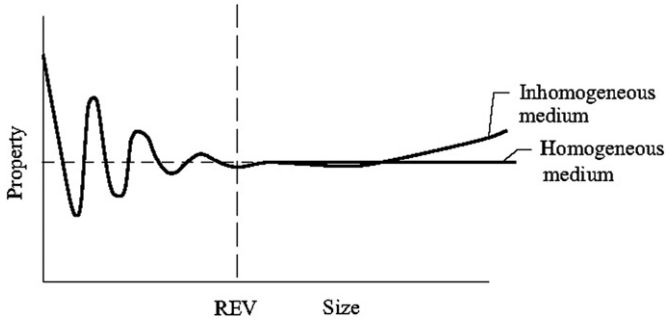

Fig. 1. The REV concept; after Hudson and Harrison [5].

Schultz [6] working with basaltic rocks at the outcrop or larger scale, suggested that the rock mass REV size is 5–10 times greater than the mean joint spacing or block size. It should be noted

that the use of REV has been more common in hydrogeology than in rock engineering [7]. In another case study, Pariseau et al. [8] faced with large computational times while running a finite element model for a rock slope used REV techniques to facilitate model execution. In this study, the selected REV size was defined as a cube with edge length 10 times the maximum joint set spacing. To this block size, more joints were added until the equivalent properties did not change significantly with further joint addition. From an engineering perspective a different rock mass property REV maybe necessary depending on the engineering problem to be solved.

Recent developments in numerical methods can be used to simulate a fractured rock mass and estimate its behavior under load. The question on the best way to introduce and interpret fracture system behavior in numerical stress analysis models has not yet been resolved. In practice the mechanical properties of fractured rock masses can be determined by using both continuum and discontinuum numerical methods. The equivalent continuum approaches, and in particular finite element techniques, have been used to determine the REV mechanical properties of several size fractured rock mass samples [8–10]. The REV size corresponds to the minimum sample size beyond which, the calculated values of the elastic properties of the specific rock mass stop fluctuating. Once a REV size is determined, modeling of jointed rock mass problems at a scale equivalent or larger than that of REV, is possible using equivalent homogeneous properties.

The discontinuous deformation method (DDM) or the distinct element method (DEM) can also be used to model the jointed rock masses. Both approaches consider a jointed rock mass as assemblies of individual blocks defined by fracture systems. The mechanical behavior of a rock mass is governed by the interaction of the intact rock blocks and fractures. The DDM and the DEM have been successfully employed to investigate the influence of scale effects on the mechanical behavior of rock masses [11,12]. Min and Jing [13] used a fracture system model coupled with a distinct element model to determine the REV size of a rock mass.

It is accepted that the complexity of a rock mass can be captured by fracture system models, generated from structural fracture sets. Grenon et al. [14] used field data from an underground mine drift to generate a 3D fracture system which was linked to a 2D distinct element stress analysis package, UDEC [15]. A series of 2D trace planes, along the simulated rock mass, were extracted from the 3D fracture system and introduced into UDEC. Although this analysis was successful in providing an understanding of the influence of structure in a stress model, it had some inherent limitations. The model did not represent fractures terminating into intact rock, so only fractures creating blocks were considered during the analysis. This could have been overcome to some extent using Voronoi blocks or by ‘‘extending’’ fractures. These approaches however, are cumbersome and not easily implemented. Another limitation is that when a set of 2D fracture traces are extracted from a 3D fracture system and are embedded into a 2D stress model like UDEC, the strength of the resulting rock mass is under-represented. Staub et al. [16] also report a similar application of a fracture system linked to UDEC, while Park et al. [17] report on extracting 2D trace sections from a 3D fracture model for the Äspö ZEDEX tunnel and integrating them in a PFC2D [18] model.

Some of the earlier efforts linking 3D fracture systems with 3D stress analysis packages have been reported by Kulatilake et al. [19] and Olofsson and Fredriksson [20] where a 3D fracture system was linked to the 3D distinct element model (3DEC) developed by Itasca [21]. In order to overcome computational limitations, Kulatilake et al. [19] limited the maximum number of fractures linked to their 3DEC model to 16. This was a considerable simplification considering that 8100 fractures were generated in the 3D fracture system model of a 30 m cubic rock mass. Furthermore, in order to be able to discretize the domain into polyhedral, as required by 3DEC, it was necessary to introduce fictitious fractures in the generated rock mass which were used in tandem with the actual fractures. This was a clever way to overcome inherent software limitations. Olofsson and Fredriksson [20] extracted 2D fracture traces from a 3D fracture model in order to derive the necessary input data for a 3DEC model which was subsequently loaded under plain strain conditions. Although innovative at the time, these approaches provide limited integration between 3D fracture system models and 3D stress analysis packages.

An interesting development is the use of the synthetic rock mass (SRM) approach to link fracture systems to PFC3D models [22]. Engineering applications include investigations on the interaction of stress and structure on the stability of vertical excavations [23] and the influence of scale effects on the calculated mechanical properties of rock masses [24–26]. An advantage of using particle flow code over some other distinct element models is the possibility to simulate fracture propagation in the rock mass. This can result in breaking of rock bridges and the creation of smaller rock blocks in the rock mass.

This paper draws from on-going investigations on ore pass performance at Brunswick Mine. The synthetic rock mass approach was used to estimate the rock mass strength and deformability of an area of interest at the mine. Based on site investigations, geological structural data were collected and used to construct a large scale fracture system model in a massive sulphide rock mass. The developed fracture system was randomly sampled, at different locations and for different sample sizes. Subsequently, the jointed rock mass samples were coupled to a PFC3D stress analysis model in order to estimate their strength and deformation behavior.

2 GENERATION OF A FRACTURE SYSTEM MODEL

2.1 Collection of structural data

A data collection campaign was undertaken at Brunswick Mine, located in northeastern New Brunswick, Canada, 26 km south-west of Bathurst. This underground lead–zinc–copper– silver mine, operated by Xstrata Zinc, has been in operation since 1964 and produces almost 10,000 tonnes/day. The ore body consists of close to ten sub-parallel massive sulphide lenses striking north–south and dipping 751 to the west. The overall strike length of the ore body is 1200 m with a width of up to 200 m. The ore body extends from surface to a depth of close to 1200 m.

The Brunswick deposit is hosted by metamorphosed volcaniclastic sediments and tuffs which overlie felsic volcanic rocks. Sharp mechanical contrasts exist between the massive sulphide which is heavy (specific gravity of 4.3), stiff and strong (UCS up to 200 MPa) and the meta-sediments. The latter are much lighter with a specific gravity of 2.6 and weaker with UCS closer to 70 MPa. Some of the important mine infrastructure is in the massive sulphides. Fig. 2 illustrates two massive sulphide exposures at the mine.

Six scan-lines were run in the massive sulphide exposures in the lower mine block at the Brunswick Mine. The rock mass is moderately fractured. Field observations demonstrated that there are two sub-vertical and one sub-horizontal fracture sets in the massive sulphide rock mass. The sub-vertical fracture sets are oriented relatively perpendicular to each other, striking toward the north–south and east–west directions. The identified three fracture sets are reproduced in Fig. 3.

In all, 151 fractures were mapped with only 4% of the measured fractures classified as random fractures. The dip and dip direction for each set and the fracture set characteristics are summarized in Table 1. The Fisher constant K was employed to quantify the dispersion of the orientation data around the mean value.

This was followed by calculation of the normal set spacing for each fracture set, using the acute angle between each scan-line orientation and the orientation of the line normal to the mean orientation of the fracture set. The trace length of fractures, on the rock mass exposures along the scan-lines, was measured using a 5 m steel measuring tape. Three types of termination fracture traces were recorded as intersecting the scan-lines during mapping: (a) both ends of a fracture trace were visible, (b) one end of a fracture trace was censored and (c) both ends of the fracture trace were censored. After obtaining the fracture length data, the approach reported by Villaescusa and Brown [27], attributed to Laslett [28], was used to correct the censoring bias of the sampled data. The unbiased mean trace length and standard deviation for each set is reported in Table 1.

a

b

Fig. 2. (a) Photo of massive sulphide rock mass looking north-west and (b) photo of massive sulphide rock mass looking east.

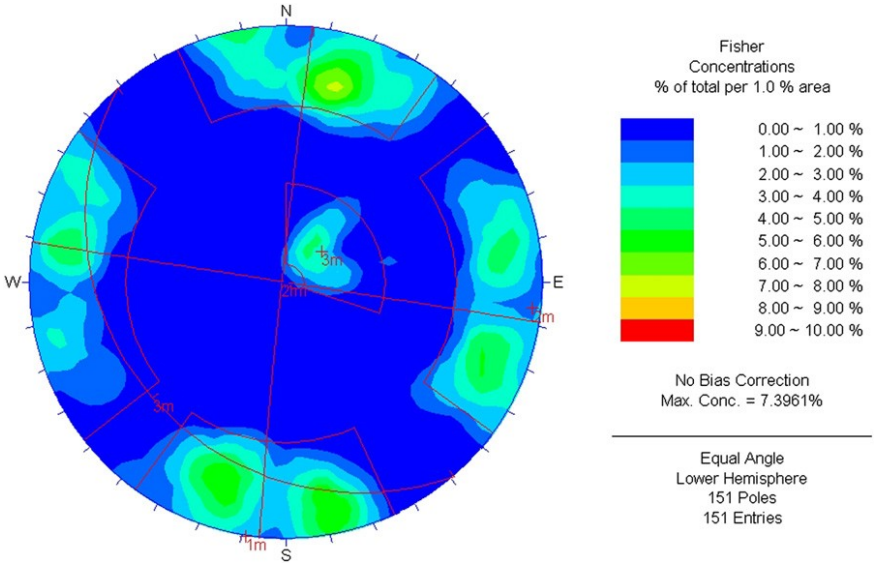

Fig. 3. Stereonet constructed from scan-line data.

Table 1. Fracture set field data and input data used for fracture system generation.

Fracture characteristic	Set #1	Set #2	Set #3
Dip (deg)	89	89	17
Dip direction (deg)	007	274	227
K	17	12	57
Spacing (m)	1.52	1.12	1.23
Std. (m)	1.8	1.0	0.8
Trace length (m)	1.40	1.44	1.16
Std. (m)	0.70	0.54	0.22
P_{32} (m^{-1})	0.98	1.55	1.09
Fracture area (m^2)	2.46	2.49	1.59

2.2 Fracture system modeling

Stochastic models provide powerful means of representing fracture systems based on available structural data. Fracture system modeling employs borehole, line mapping or face mapping field data to generate representative models of the prevailing structural conditions. Rogers et al. [29] note that early interest in the fracture systems approach was associated with nuclear waste sites while in recent years there is increased focus towards the modeling of fractured hydrocarbon reservoirs with limited use in the design of rock engineering structures in fractured rock masses.

The fundamentals of stochastic modeling are discussed in detail by Dershowitz and Einstein [30] where they demonstrate that fracture system models can be used to represent rock mass geometry as an entity. They furthermore presented detailed descriptions of the Orthogonal, Baecher, Veneziano, Dershowitz and Mosaic Tessellation models. Staub et al. [16] contributes to the discussion, by providing details on some more recent conceptual models. The various fracture system modeling tools vary in complexity and in the way they model fracture location, orientation, intensity, size, co-planarity, termination and hierarchy.

In most cases, fracture locations are stochastic. Fracture size, the trace length on two dimensional surfaces or surface area of individual fractures, is usually specified directly or indirectly through stochastic location and orientation. Most models can accommodate fractures that intersect other fractures or terminate in intact rock. Co-planarity implies that a number of fractures can be located in the same plane. Furthermore, models may account for discrete fractures intersecting the studied region. Finally, some zones with different structural properties may be defined within a FSM. Some sophisticated models interpret not only geometry but also fracture hierarchy [31].

Although conceptually elegant, the majority of models have not been adequately verified or used in rock engineering applications. In practice, the choice of the model will depend on how it can be related to the available field data and to the engineering needs of the project. Recent years have seen the development of several fracture systems generators of varying complexity and ease of use. These generators can be model specific, such as Stereoblock based on the Baecher model, Hadjigeorgiou et al. [32], or Fracture-SG which is based on the Veneziano model, Grenon and Hadjigeorgiou [33,34]. Other generators such as FracMan [35], can capture different geological environments and can be used for more diverse engineering applications.

2.3 Fracture system generation and validation

The Fracture-SG [33] generator was used for the Brunswick site. The generator is based on the Veneziano model which relies on the generation of a Poisson network of planes in 3D space followed by a secondary process of tessellation by a Poisson line process and marking of polygonal fractures.

The model is conceptually simple and is easy to use as the required input parameters can be determined based on structural mapping. The model results in polygonal shape fractures. A conceptual limitation of the Veneziano model is that fractures produced on the same plane, during the primary generation process, remain coplanar after the secondary tessellation process.

A geometric model was constructed to facilitate the creation of a realistic synthetic rock mass. Fracture generation was realized, per fracture set basis, using size, intensity and orientation as input. The model was generated based on the P_{32} for intensity and fracture area (m^2) values, reported in Table 1. The FSM was calibrated using forward modeling. The resulting three dimensional system, 40 m x 40 m x 40 m of polygonal shape fractures is illustrated in Fig. 4.

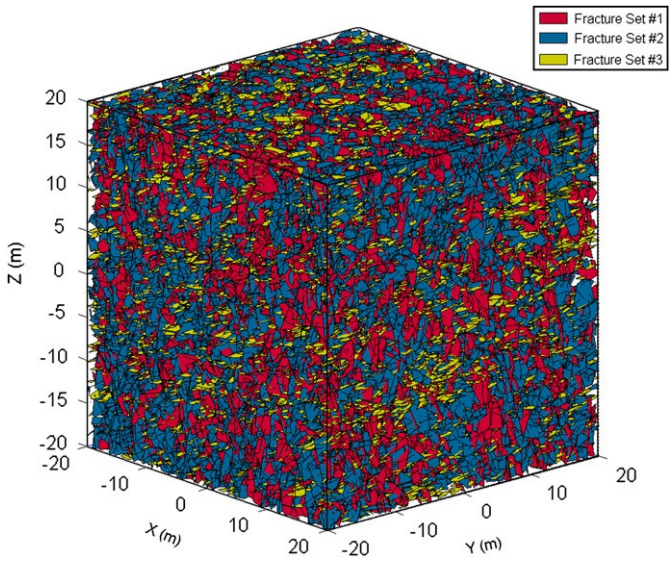

Fig. 4. Visualization of the generated fracture system. North coinciding with the Y-axis.

A fundamental concern is whether the generated fracture systems are representative of observed field conditions. This is often difficult to quantify due to the limited available field data. This was overcome by sampling the generated fracture system using simulated mapping lines and planes similar to structural field mapping. Six scan-lines, parallel to the scan-lines used during the in situ structural mapping, were introduced into the fracture system. The trace length, orientation and spacing of all fracture sets intersected by the virtual scan-lines were recorded. Subsequently, the results of the sampled virtual rock mass were compared to the collected field data.

The Kolmogorov–Smirnov test was used to compare orientation, spacing and trace length distributions of the in-situ and the modeled fracture sets. A 5% significant level was selected to accept or reject the null hypothesis that the field and simulated data are from the same distribution. This calibration process was repeated until statistical agreement was reached between the field data and simulated data. Consequently the validated FSM was accepted as a plausible representation of the in situ fracture system. Since fracture system models are based on stochastic generation, the fracture system used in this analysis is only one of many possible systems.

2.4 Sampling of the fracture system

The validated fracture system model was then subjected to random spatial sampling. In all, 40 cubic samples of constant height–width ratio of 2, and of varying base width (0.05, 0.1, 0.2, 0.5, 1.5, 3.5, 7.0, and 10.0 m) were collected, Fig. 5. For each sample size, five samples were extracted from within the initial FSM ‘‘master’’ volume. It was observed that not all generated fracture sets were present in the smaller samples. Furthermore, depending on the size and location of the samples

within the master volume, a fracture can be completely engulfed or it can be delineated (truncated) by the sample boundaries.

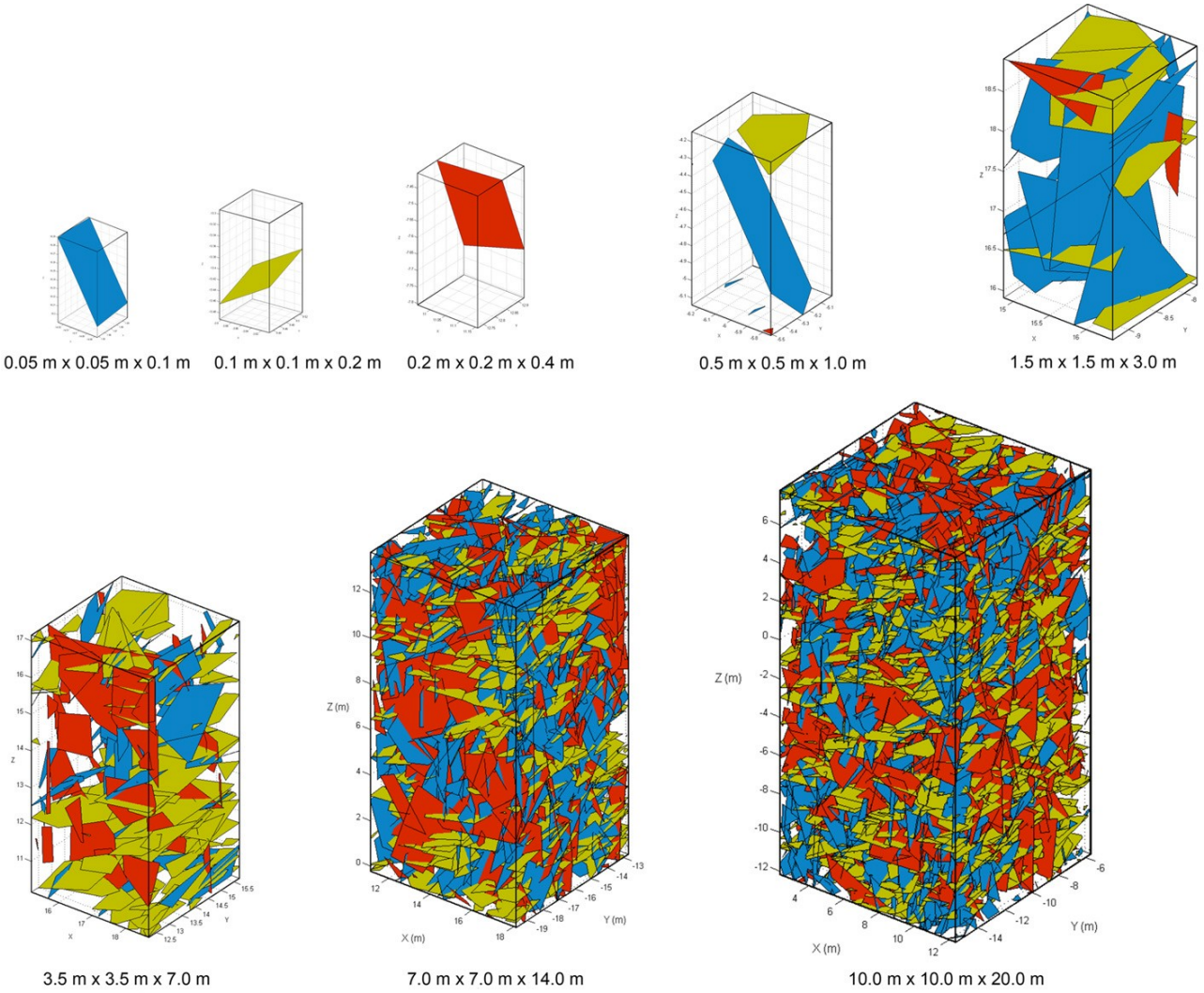

Fig. 5. Rock mass samples drawn from the fracture system model (not to scale).

3 ESTIMATION OF GEOMETRICAL BASED REV SIZE

In a jointed rock mass, the number of intersected fractures increases with sample size. The relationship between sample size and the number of fractures in each sample (P_{30}) is illustrated in Fig. 6. The same graph illustrates the observed variation in the number of fractures for each sample size. The number of intersected fractures within a sample is influenced by fracture set orientation, spacing and size.

Another way to quantify fracture intensity is the fracture area per rock volume (P_{32}). As illustrated in Fig. 7 variations in the calculated P_{32} decrease as the sample size increases. The P_{32} for this rock mass converges to a mean value of 2.65 for the 7.0 m x 7.0 m x 14.0 m sample.

The volumetric fracture intensity (P_{32}) does not depend on the fracture orientation and size distribution. As long as it is representative of the fracture system, P_{32} is independent of the size of the sampled region [36]. Fracture spacing, however, depends on fracture orientation and the orientation of the mapped rock mass exposure. Chalhoub and Pouya [9] measured the fracture

spacing along different directions in a rock mass to calculate the REV size. They reported that the REV size varied from 18 to 30 times the fracture spacing, depending on the direction of mapping. As fracture spacing is not isotropic, it follows that REV size should then be quantified on a directional basis.

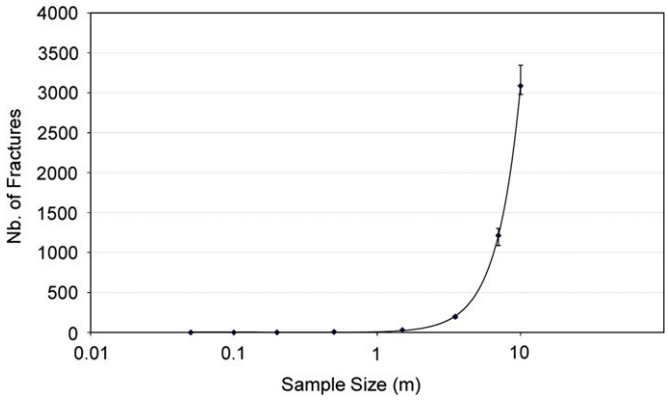

Fig. 6. Relationship between sample size and number of fractures, including variations.

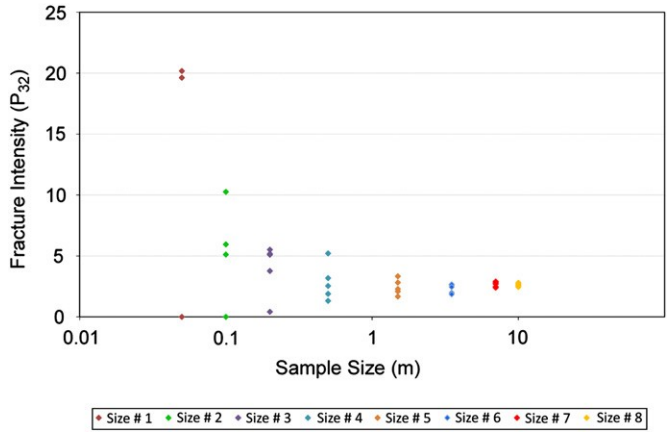

Fig. 7. Fracture intensity (P32) of different sample sizes.

Table 2. The results of T-test and F-test for fracture intensity P32.

Sample size (m)	*T*-test		*F*-test	
	P-value	Results	*P*-value	Results
0.05	0.33	Accepted	1.4e−7	Rejected
0.1	0.44	Accepted	5.5e−6	Rejected
0.2	0.22	Accepted	1.02e−4	Rejected
0.5	0.79	Accepted	3.8e−4	Rejected
1.5	0.51	Accepted	0.01	Rejected
3.5	0.11	Accepted	0.07	Accepted
7	0.77	Accepted	0.4	Accepted

The T and F statistical tests were performed to quantify REV size based on fracture intensity (P_{32}) for different sample sizes. The T-test (Student test) assesses whether the means of two groups are

statistically different from each other. In this analysis the mean P_{32} value for the 10 m sample was compared with the P_{32} means for the smaller samples. The T-test was used to investigate the null hypothesis that data in both groups (i.e. sample sizes) were independent random samples from normal distributions with equal means and unknown variances. This was tested against the alternative hypothesis that the means were not equal.

The F-test was used to determine whether the variances of the calculated P_{32} for different sample sizes, were statistically different from the 10 m sample. An F-test was performed to validate the null hypothesis that two independent samples were from normal distributions with the same variance, against the alternative that they were from a normal distributions with different variances.

The results of the T-test and F-test for fracture intensity are summarized in Table 2. All calculations were based on a maximum significant level of 5%. The maximum significant level at which the null hypothesis cannot be rejected is the P-value. The higher the P-value, the more probable the mean values and variances of different sample sizes are equal.

The T-test demonstrated that the null hypothesis (the mean values being equal) could not be rejected at the 5% significant level, while the results of the F-test showed that the sample variance was equal when the sample size reached a width of 3.5 m. In this example the P_{32} based REV size, defined by an equal mean and variance values for different sample sizes, was 3.5 m.

4 GENERATION OF SYNTHETIC ROCK MASS SAMPLES

The preceding sections reviewed the generated 3D fracture systems models which were used to suggest an appropriate REV value based on P_{32}. In order to predict the mechanical behavior of the FSM rock masses it is necessary to load these large samples. An interesting approach to tackle this problem is the use of ‘‘synthetic rock mass models’’ (SRM) whereby a jointed rock mass is represented as an assembly of fractures inserted into a rock matrix. A practical way to accomplish this goal is by linking a fracture system model to a bonded particle model. A bonded particle model was constructed using the 3D particle flow code (PFC3D), [37]. An intact rock was simulated as an assembly of rigid distinct spherical particles, bonded together at their contact points. A linear contact and a frictional sliding model were used to describe the physical behavior of the contacts. Finally a disk-shaped fracture system was superimposed on this synthetic rock, which was then put under load.

4.1 Intact rock properties

The intact rock samples were generated using procedures developed by Potyondy and Cundall [38]. A bonded particle model is characterized by the density, shape, size distribution, assembly and the micro-properties of constituent particles and bonds. The macroscopic mechanical properties of an intact rock sample can be developed by several combinations of micro-mechanical properties. For the purposes of this work the geomechanical database of Brunswick Mine was used to provide the mechanical properties of intact rock samples. An inverse calibration method was used to establish the necessary micro-mechanical parameters that would replicate the representative intact rock properties.

The first parameter defined at the macro level was the elastic modulus. In the PFC model the elastic modulus is controlled by particle contact modulus E_c, particle normal/shear stiffness (k_n/k_s), parallel bond modulus $\bar{E}_c$ and bond normal/shear stiffness ($\bar{k}_n/\bar{k}_s$). Once the desired elastic secant modulus was achieved, Poisson’s ratio of the PFC material was determined. These values were influenced by the choice of particle normal/shear stiffness (k_n/k_s) and bond normal/shear stiffness ($\bar{k}_n/\bar{k}_s$) ratios. The last stage in this iterative process was the determination of the uniaxial strength of the intact rock. This strength value is controlled by the average normal and shear strengths of the particle bonds.

The micro-mechanical properties of particles and bonds used to generate the bonded particle model of intact rock are summarized in Table 3. The laboratory-derived mechanical properties for intact rock samples in the massive sulphides are summarized in Table 4. These laboratory values provided the starting point for the calibration process using PFC3D. The calibrated results for intact rock are also reported in Table 4. The bonded particle models were calibrated to validate the average mechanical properties of the intact rock measured in the laboratory. This investigation did not consider the possibility of an intact rock scale effect.

Table 3. Micro-properties of the PFC3D models.

Sample size (m)	R_{min} (cm)	E_c (GPa)	$\sigma = \tau$ (MPa)	Std. (MPa)
0.05	0.16	117	189	45
0.1	0.31	112	183	45
0.2	0.6	119	181	45
0.5	1.4	114	167	45
1.5	2.5	123	162	45
3.5	3.6	122	151	45
7.0	7.0	121	140	45
10.0	10	120	130	45

R_{min}: minimum particle radius.
E_c: particle contact and parallel bond modulus.
σ: bond normal strength.
τ: bond shear strength.
Std.: standard deviation of bond normal and shear strength.

Table 4. Mechanical properties of intact rock and calibrated bonded particle models.

Mechanical properties	UCS (MPa)	E (GPa)	Poisson ratio	Specific gravity
Massive sulphide	205	104	0.29	4.3
PFC3D samples (m)				
0.05	203	104	0.29	4.3
0.1	204	102	0.29	4.3
0.2	205	104	0.27	4.3
0.5	204	103	0.28	4.3
1.5	205	104	0.28	4.3
3.5	204	104	0.27	4.3
7.0	204	105	0.29	4.3
10.0	205	103	0.28	4.3

The construction and calibration of large intact rock samples in PFC3D imposes high computational requirements. In order to overcome this obstacle the calibration process was simplified for the larger samples, using the pre-compacted bricks approach proposed by Mas Ivars et al. [26]. Bricks were assembled together to construct rapidly the large intact samples. In this study 0.5 m width bricks were used for the 1.5 m sample, 0.7 m for the 3.5 m, 1.4 m for the 7.0 and 2 m for the 10 m sample. The particle friction coefficient was fixed at 2.5 and the ratio of particle and bond normal to shear stiffness was equal to 3.6 for all samples.

4.2 Fracture properties

The introduction of fractures in a PFC model has been somewhat problematic in the past because of the inherent roughness (bumpiness) of the interface surfaces. In earlier versions of the PFC, fractures were represented by a band of low-strength material. Consequently, particles that fell along opposite sides of a fracture plane were forced to move around each other in order to slide. This work took advantage of the smooth joint model (SJM) option which was applied to particle contacts. The SJM is a major improvement over prior versions of the PFC software as it simulates the behavior of an interface, regardless of local particle contact orientations along the interface. This ensures sliding and unraveling of rock blocks along the fracture surface [39].

For the purposes of this study all fractures were assumed to be cohesionless and having an angle of friction of 30°. The calibration process described by Hadjigeorgiou et al. [23] was used to assign the necessary micro-mechanical properties to the particles along the fracture planes, in order to achieve the desired macro-properties. This was done by conducting a series of triaxial tests in the PFC3D model. Four specimens, each intersected by a fracture at a different inclination of 45°, 50°, 55°, and 60° were tested under a confinement stress of 1 MPa. The axial stress, initiating sliding along the fracture surface, was recorded during each test. In designing these tests, the bond strength along the fracture surface was set to zero, and a range of coefficients of friction of adjacent particles (0.1, 0.15, 0.2, 0.25, and 0.3) along a fracture plane were used to arrive at the desired strength. Based on these iterations a coefficients of friction of adjacent particles of 0.2 resulted in zero cohesion and an angle of friction of 30° for the fractures. Another part of the iteration process involved selecting appropriate normal and shear stiffness for the particles along the fracture surface. An initial stiffness value was selected based on the elastic modulus and average particle size. Following a series of iteration a value of 2.5×10^{12} N/m^3 was selected for the normal stiffness and 0.5×10^{12} N/m^3 for the shear stiffness of particles along the fracture surfaces.

These calibration exercises resulted in fractures in the synthetic rock mass samples with the desired macro-mechanical properties of zero cohesion and an angle of friction of 30°. This configuration facilitated the generation of the desired macro-mechanical properties of the fractures. The same mechanical properties were assigned to all fractures in the synthetic rock mass although it is acknowledged that the peak shear strength of fractures can decrease as fracture size increases [40].

4.3 Sample generation

The micro-mechanical properties in Table 3 were used to generate rock samples in PFC3D-V.4.0 [37]. These are illustrated in Fig. 8 and the number of particles used to generate the different sample sizes listed in Table 5. Once the intact rock samples were generated, all fractures generated using Fracture-SG [33] were introduced in the corresponding bonded particle models.

The generated fracture system using Fracture-SG and illustrated in Fig. 4 is based on the Veneziano model which results in polygonal shape fractures. In PFC3D, however, fractures are represented as disk shape features, identified by their center point and radius.

Consequently, it was necessary to approximate the generated polygonal fractures as disks. This was done using the fracture center point and its equivalent radius. FISH-Lab [41] developed by

Itasca was used to visualize the constructed fracture systems in the synthetic rock samples, Fig. 9. The influence of sample size on the number of encountered fractures is evident.

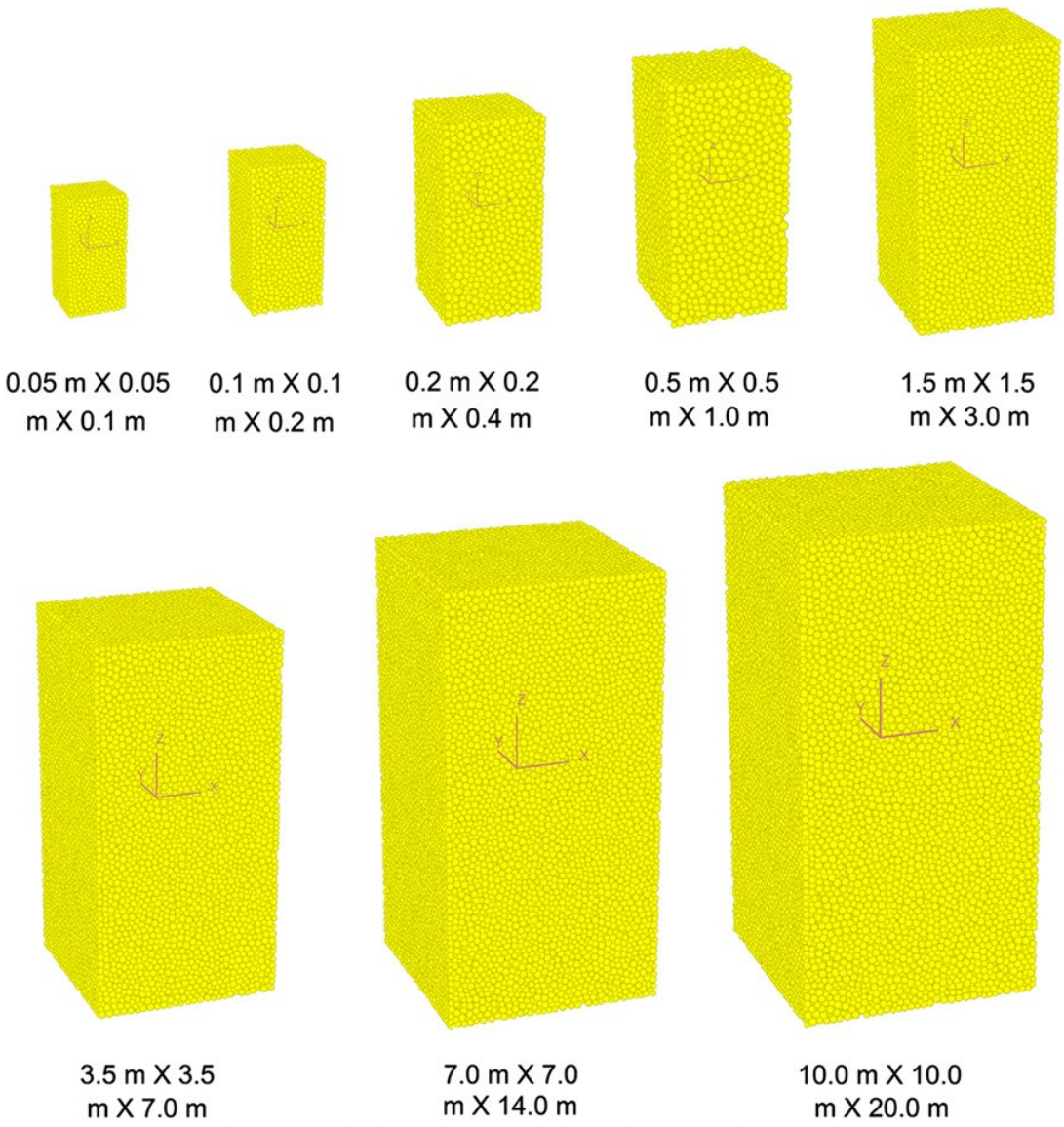

Fig.8. Bonded particle models of intact rock samples.

Table 5. Number of particles in different sample size.

Sample size (m)	No. of particles	Sample size (m)	No. of particles
0.05	5512	1.5	39,014
0.1	6063	3.5	92,300
0.2	6689	7.0	115,455
0.5	8228	10.0	142,376

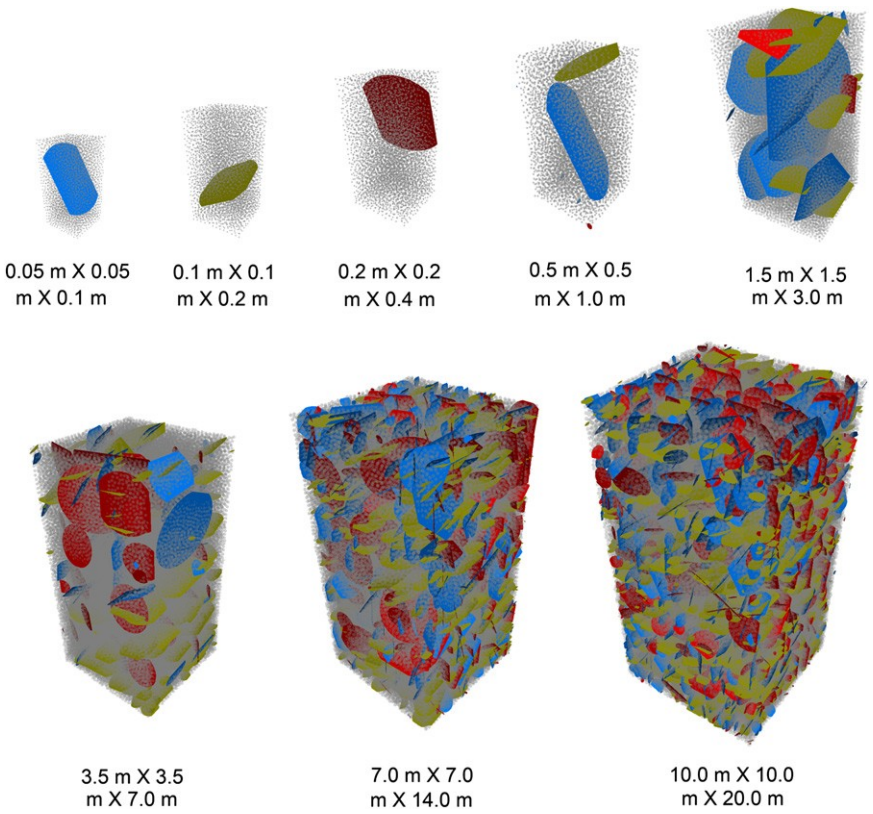

Fig. 9. Synthetic rock mass samples generated by linking the PFC3D and fracture system models.

4.4 Uniaxial compressive test of synthetic rock samples

A series of uniaxial compressive tests were performed on all 40 synthetic rock mass samples. The PFC3D code was run on a computer using a Pentium IV processor with a speed of 3.3 GHz. The wall-based loading procedure in PFC3D was used to load the 0.05, 0.1, 0.2, and 0.5 m synthetic rock mass samples. In this process, the walls that confine the specimen in the bonded particle model generation were used to load the specimen with the top and bottom walls acting as loading platens, Fig. 10a. In order to speed up the testing of large samples the authors employed a testing methodology developed by Itasca [37] that uses particles as boundaries. This approach facilitates uniaxial, triaxial, and direct tension testing of large sample sizes along different coordinate directions. A grip-based procedure and a rapid loading methodology were used for the larger samples. Grip spheres on the top and bottom of each synthetic rock mass sample were identified as plates and loading was performed using internal-based or platen-based methods. Internal-based loading methods assign linearly varying axial velocities to all assembly particles. This can result in a specified gradual development of induced axial strain in the assembly of particles over a certain number of calculation steps. At each induced strain stage, the grip particles are stopped, the axial velocity of all other particles is set to zero and they are free to move until static equilibrium is re-established. The platen-based approach is performed by moving the grip platens toward one another to obtain the desired velocity of the grip spheres. This platen-based approach was used to load the larger synthetic rock mass samples shown in Fig. 10b. Two of the larger samples, defined by a base width of 7 and 10 m, were randomly selected for comparing the results of both loading methods. The results obtained by the platen-based and internal-based methods were very close, less than 2 MPa apart.

What is important in both the platen and grip based approaches, is the loading rate applied to the particle assembly. This must be sufficiently slow in order to allow time for the particle assembly to adjust to the force redistribution that accompanies slip and bond breakage.

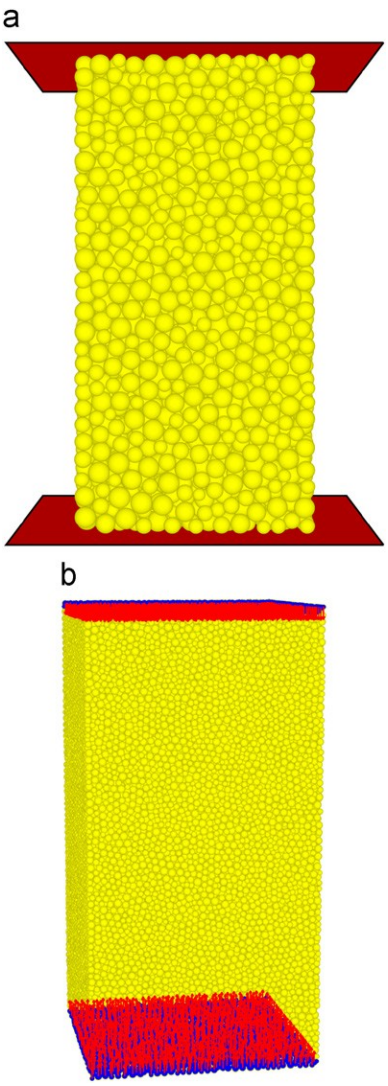

Fig. 10. Uniaxial compressive test of synthetic samples: (a) using wall for loading and (b) using spherical grip particles for loading.

4.5 Strength of a jointed rock mass

The relationship between sample size and normalized uniaxial compressive strength (UCS of tested samples/UCS of intact rock), calculated from the PFC3D loading tests is illustrated in Fig. 11. This includes the 90% confidence limits. The average strength, for the smallest sample of 0.05 m, was approximately 160 MPa. This is somewhat lower than the uniaxial strength of the intact rock. At the other extreme, the average strength of the 10 m x 10 m x 20 m rock mass sample (size #8) was approximately 45 MPa. This is close to 0.20 of the UCS of the intact rock.

The T and F tests were used to analyze the uniaxial compressive strength results obtained for the different samples. The mean and variance of the 10 m sample size were compared with that of the smaller sample sizes. The F-test results, summarized in Table 6, show that the sample variances

are equal only when the sample size reaches 7 m with samples smaller than 7 m displaying a much larger variance.

The T-test indicates if the null hypothesis (i.e.: the mean values are equal) can be rejected at the 5% significant level. For the smallest size sample the mean UCS value is higher. The higher mean value and variation for the smallest sample is attributed to the very small number of fractures present. This can result in failure of the rock samples along several possible continuous preferential planes of weaknesses or through intact rock. For the mid-range sample sizes, T-test indicates that the null hypothesis cannot be rejected due to the high variances of uniaxial test results of these samples. For the 3.5 m size samples the mean UCS value is higher than for the 10 m size samples and for the 7.0 m samples the null hypothesis cannot be rejected.

Mean UCS and variance decrease with sample size. The REV size, defined by an equal mean and variance values for different sample sizes, is 7 m based on UCS values.

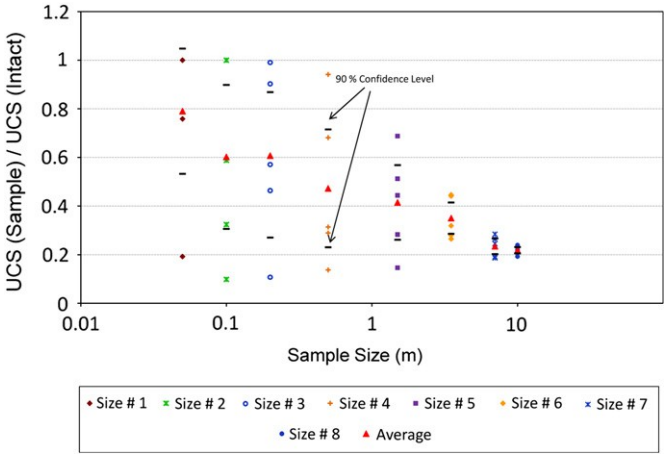

Fig. 11. Influence of specimen size on the strength of rock mass.

Table 6. The results of T-test and F-test for the UCS of the synthetic rock mass samples.

Sample size	*T*-test		*F*-test	
	P-value	Test result	*P*-value	Test result
0.05	0.02	Rejected	4.2e–5	Rejected
0.1	0.10	Accepted	2.3e–5	Rejected
0.2	0.07	Accepted	3.8e–5	Rejected
0.5	0.16	Accepted	5.2e–5	Rejected
1.5	0.10	Accepted	3.1e-4	Rejected
3.5	0.02	Rejected	0.0095	Rejected
7	0.49	Accepted	0.11	Accepted

4.6 Deformability of fractured rock mass

The elastic modulus of synthetic rock mass samples was measured during the uniaxial loading tests. Fig. 12 presents the normalized elastic modulus (elastic modulus of tested samples/ elastic modulus of intact rock) versus sample size. The 90% confidence limit illustrates that, the elastic modulus for the largest sample size is about 0.35–0.4 of the intact rock elastic modulus. The average

elastic modulus for the smallest sample of 0.05 m in width was close to 90 GPa, while for the largest sample of 10 m width it was about 38 GPa.

Both the T and F tests were used to analyze the elastic modulus (E) data where the mean and variance of the largest size sample was compared with that of smaller samples. The results are summarized in Table 7.

Based on the F-test, sample variances are equal only for the 7 m width samples. Below that sample size, variances are larger. The results from the T-test demonstrate that for the three smaller sample sizes (0.05, 0.1, and 0.2 m), the mean E values are higher than for the 10 m sample. Based on the large observed variances the null hypothesis could not be rejected for the 0.5 and 1.5 m samples. The mean E value of the 3.5 m size samples is higher than the 10 m size samples. The null hypothesis cannot be rejected for the 7.0 m samples. In general the mean elastic modulus and variance decrease with sample size and in this study the elastic modulus based REV size was selected as 7 m.

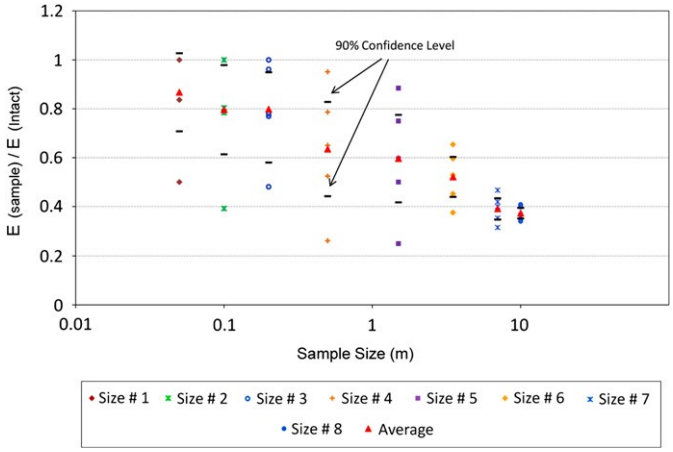

Fig. 12. Influence of specimen size on the elastic modulus of rock mass.

Table 7. The results of T-test and F-test for the elastic modulus of the synthetic rock mass samples.

Sample size	*T*-test		*F*-test	
	P-value	Test result	*P*-value	Test result
0.05	0.0064	Rejected	1.9e−3	Rejected
0.1	0.018	Rejected	1.2e−3	Rejected
0.2	0.009	Rejected	2.3e−3	Rejected
0.5	0.088	Accepted	9.4e−4	Rejected
1.5	0.10	Accepted	0.0012	Rejected
3.5	0.035	Rejected	0.024	Rejected
7	0.42	Accepted	0.2	Accepted

5 DISCUSSION

The coefficient of variation (CV), the ratio of the standard deviation to the mean value, was used to select appropriate REV size for the selected rock mass. The coefficient of variation of the mechanical properties (UCS and E) and geometrical properties (number of fractures and P_{32}) were plotted against sample size, Fig. 13.

The geometrical properties of the rock mass samples are listed in Table 8 while the mechanical properties are listed in Table 9.

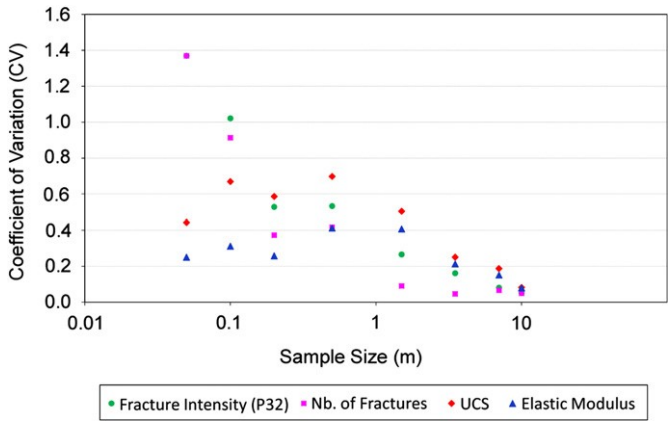

Fig. 13. Coefficient of variation versus sample size.

Table 8. Results of geometrical rock mass characterization.

Sample size (m)	Number of fractures					Mean value	Std.	Fracture intensity (P_{32}) (m^{-1})					Mean value (m^{-1})	Std. (m^{-1})
	S1	S2	S3	S4	S5			S1	S2	S3	S4	S5		
0.05	1	0	1	0	0	0.4	0.5	20.1	0.00	19.6	0.00	0.00	7.96	10.90
0.1	0	1	0	1	1	0.6	0.5	0.00	5.11	0.00	10.26	5.95	4.26	4.35
0.2	1	1	1	2	1	1.2	0.4	3.76	5.09	0.41	5.51	5.18	3.99	2.10
0.5	10	5	3	7	6	6.2	2.6	5.21	3.18	1.31	1.88	2.53	2.82	1.50
1.5	34	28	33	28	31	30.8	2.7	3.33	2.81	2.08	2.28	1.66	2.43	0.64
3.5	198	203	205	182	199	197.4	9.0	1.97	2.60	2.66	1.84	2.45	2.30	0.37
7	1232	1090	1304	1194	1252	1214.4	80.0	2.80	2.40	2.90	2.47	2.70	2.65	0.21
10	2986	3026	2980	3098	3346	3087.2	152.1	2.55	2.70	2.45	2.60	2.80	2.62	0.13

Table 9. Results of mechanical rock mass characterization.

Sample size (m)	UCS of intact rock (MPa)	Elastic modulus of intact rock (GPa)	Uniaxial compressive strength of synthetic rock masses (MPa)					Mean value (MPa)	Std. (MPa)	Elastic modulus of synthetic rock masses (GPa)					Mean value (GPa)	Std. (GPa)
			S1	S2	S3	S4	S5			S1	S2	S3	S4	S5		
0.05	203	104	154	203	39	203	203	160.4	71.1	87	104	52	104	104	90.2	22.5
0.1	204	102	204	66	204	120	20	122.8	82.1	102	82	102	80	40	81.2	25.3
0.2	205	104	95	185	203	22	117	124.4	72.8	80	100	104	50	81	83.0	21.4
0.5	204	103	28	139	192	64	59	96.4	67.2	27	81	98	67	54	65.4	26.9
1.5	205	104	30	58	91	105	141	85.0	42.7	26	52	62	78	92	62.0	25.2
3.5	204	104	90	57	65	91	54	71.4	17.8	62	55	47	68	39	54.2	11.5
7	204	105	38	54	39	58	50	47.8	8.9	33	44	37	49	42	41.0	6.2
10	205	103	45	49	47	39.5	43	44.7	3.6	38	42	41	36	35	38.4	3.0

Table 10. Determination of REV size of rock mass based on coefficient of variation.

Acceptable coefficient of variation (%)	Geometrical REV	Mechanical REV	Geometrical and mechanical REV
< 20	3.5 m × 3.5 m × 7 m	7 m × 7 m × 14 m	7 m × 7 m × 14 m
< 10	7 m × 7 m × 7 m	10 m × 10 m × 20 m	10 m × 10 m × 20 m

It is noted that some of the smaller size samples, such as the 0.05 and 0.1 m, did not contain any fractures. In other words, for all practical purposes, these were intact rock samples. Consequently, when tested they recorded much higher UCS values, Table 9. This explains the somewhat lower coefficient of variation for the mechanical properties of these sample sizes.

It is interesting to observe that the coefficient of variation values, for both mechanical and geometrical properties, converge when the sample size has a width dimension between 3.5 and 7 m. Min and Jing [13] had suggested that the REV size for a given rock mass can be determined according to a chosen ‘‘acceptable variation’’. In this study, following the proposed guidelines, the acceptable variations for CV were 10% and 20%. The selected REV sizes, for both mechanical and geometrical properties based on these criteria are summarized in Table 10. If only the geometrical properties were considered the selected REV would be 3.5 m. If the decision is based on the mechanical properties of the rock mass then a 7 m REV size is a more appropriate choice.

The REV sizes based on the coefficient of variation criteria and the T and F tests are close. In this case study, based on the available conditions the rock mass can be described by a global REV size, considering both geometrical and mechanical properties, of 7 m x 7 m x 14 m.

6 CONCLUSIONS

This paper presented a quantitative procedure to estimate REV size for an area in massive sulphides at the Brunswick Mine. Field data were collected to construct representative fracture systems. A sampling strategy was implemented within the FSM and the generated fracture systems were introduced into bonded particle models to construct the synthetic rock mass samples. All generated rock mass samples were loaded under a uniaxial compressive force. The number of fractures in each sample volume (P_{30}) and the volumetric fracture intensity (P_{32}) of the samples were used to provide a comprehensive characterization of the structural complexity of the rock mass. The mechanical properties of the rock mass samples were determined by a series of numerical experiments to determine the compressive strength (UCS) and elastic modulus (E) of the synthetic rock mass samples.

The REV size of the selected rock mass properties were determined using the T-test and F-test and by plotting the coefficient of variation against the sample size. Both approaches suggest that in this particular site the geometrical REV size is 3.5 m x 3.5 mx 7 m. The mechanical REV size was 7 m x 7m x 14 m. Consequently, the largest REV constitutes the global REV for this site beyond which both the mechanical and geometrical properties of the rock mass are reasonably consistent with repeated testing.

The REV size obtained for the massive sulphide rock mass at the Brunswick Mine implies that for large scale excavations such as mining stopes, the equivalent continuum approach can be used in the selection of appropriate numerical models. In these cases, the REV-derived mechanical behavior can be employed as input data for the massive sulphide rock mass. The SRM-derived mechanical properties can be used as input parameters for the mine scale global numerical stress analysis simulations that are frequently used at Brunswick Mine.

On the other hand, when the scale of excavation size versus rock mass block size is small, such as ore passes, drifts, etc. the equivalent continuum approach is not applicable. The results reported in this paper were used for a stability analysis of an ore pass system at the mine. As the employed tools are becoming more accessible then it is possible that these techniques will be used more often for a range of mine design applications. Future developments will be aided by improved data collection techniques that will capture the quality data necessary to generate the fracture systems and improved computational tools that will facilitate the time of data integration and time of execution.

ACKNOWLEDGEMENTS

The authors would like to acknowledge the support of the Natural Science and Engineering Research Council of Canada and Brunswick Mine of Xstrata Zinc.

REFERENCES

[1] Krauland N, Soder P, Agmalm G. Determination of rock mass strength by rock mass classification—some experience and questions from boliden mines. Int J Rock Mech Min Sci 1989;26:115–23.
[2] Schultz R. Limits on strength and deformation properties of jointed basaltic rock masses. Rock Mech Rock Eng 1995;28:1–15.
[3] Justo JL, Justo E, Azanon JM. The use of rock mass classification systems to estimate the modulus and strength of jointed rock. Rock Mech Rock Eng 2009, doi:10.1007/s00603-009-0040-6.
[4] Heuze F. Scale effects in the determination of rock mass strength and deformability. Rock Mech 1980;12:167–92.
[5] Hudson JA, Harrison JP. Engineering rock mechanics. Oxford: Elsevier; 1997.
[6] Schultz R. Relative scale and the strength and deformability of rock masses. J Struct Geol 1996;18:1139–49.
[7] Chen SH, Feng XM, Isam S. Numerical estimation of REV and permeability tensor for fractured rock masses by composite element method. Int J Num Anal Methods 2008;32:1459–77.
[8] Pariseau W, Puri S, Schmelter S. A new model for effects of impersistent joint set on rock slope stability. Int J Rock Mech Min Sci 2008;45:122–31.
[9] Chalhoub M, Pouya A. Numerical homogenization of a fractured rock mass: a geometrical approach to determine the mechanical representative elementary volume. Electron J Geotech Eng 2008;13. (Bund. K).
[10] Pouya A, Ghoreychi M. Determination of rock mass strength properties by homogenization. Int J Numer Anal Methods 2001;25:1285–303.
[11] Castelli M, Saetta V, Scavia C. Numerical study of scale effects on the stiffness modulus of rock masses. Int J Geomech 2003;3:160–9.
[12] PHSW Kulatilake, Wang S, Stephansson O. Effect of finite size joints on the deformability of jointed rock in three dimensions. Int J Rock Mech Min Sci Geomech Abstr 1993;30:479–501.
[13] Min KB, Jing L. Numerical determination of the equivalent elastic compliance tensor for fractured rock masses using the distinct element method. Int J Rock Mech Min Sci 2003;40:795–816.
[14] Grenon M, Hadjigeorgiou J, Harrison JP. Drift stability in moderately jointed rock. CIM Bull 2001;94:74–9.
[15] Itasca. Universal distinct element code (UDEC). Itasca Consulting Group, Inc.; 1996.
[16] Staub I, Fredriksson A, Outters N. Strategy for a rock mechanics site descriptive model. SKB report R-02-02, Swedish Nuclear Fuel and Waste Management Co., Stockholm, 2002.
[17] Park ES, Martin CD, Christiansson R. Simulation of the mechanical behavior of discontinuous rock masses using a bonded particle model. In: Proceeding of the Gulf Rock, the sixth North American rock mechanics symposium, Houston, TX, 2004.
[18] Itasca. Two dimensional particle flow code (PFC2D). Itasca Consulting Group, Inc.; 1999.
[19] Kulatilake PHSW, Park J, UM J. Estimation of rock mass strength and deformability in 3D for a 30 m cube at a depth of 458 m at A¨ spoˆ Hard Rock
Laboratory. Geotech Geol Eng 2004;22:313–30.
[20] Olofsson I, Fredriksson A. Strategy for a numerical rock mechanics site descriptive model: future development of the theoretical/numerical approach. SKB report R-05-43. Stockholm: Swedish Nuclear Fuel and Waste Management Co.; 2005.
[21] Itasca. Three dimensional distinct element code (3DEC). Itasca Consulting Group, Inc.; 2003.
[22] Pierce M, Mas Ivars D, Cundall PA, Potyondy D. A synthetic rock mass model for jointed rock. In: Proceedings of the first CA-US rock mechanics symposium, Vancouver, BC, 2007. p. 341–9.
[23] Hadjigeorgiou J, Esmaieli K, Grenon M. Stability analysis of vertical excavations in hard rock by integrating a fracture system into a PFC model. Tunn Undergr Sp Tech 2009;24:296–308.

[24] Esmaieli K, Hadjigeorgiou J, Grenon M. Estimation of synthetic rock mass strength accounting for sample size. In: Proceeding of the international conference on rock joints and jointed rock masses, Tucson, AZ, 2009.
[25] Cundall PA, Pierce M, Mas Ivars D. Quantifying the size effect of rock mass strength. In: Proceeding of the first southern hemisphere international rock mechanics symposium, Perth, Western Australia, 2008. p. 3–15.
[26] Mas Ivars D, Pierce M, DeGagne D, Darcel C. Anisotropy and scale dependency in jointed rock mass strength—a synthetic rock mass study. In: Proceedings of the first international FLAC/DEM symposium, paper no. 06-01, Minneapolis, MN, 2008.
[27] Villaescusa E, Brown ET. Maximum likelihood estimation of fracture size from trace length measurements. Rock Mech Rock Eng 1992;25: 67–87.
[28] Laslett GM. Censoring and edge effects in areal and line transect sampling of rock joint traces. Math Geol 1982;14:125–40.
[29] Rogers S, Moffitt K, Chance A. Using realistic fracture network models for modeling block stability and groundwater flow in rock slopes. In: Canadian geotechnical conference, Vancouver, BC, 2006. p. 1452–9.
[30] Dershowitz WS, Einstein HH. Characterizing rock joint geometry with joint system models. Rock Mech Rock Eng 1988;21:21–51.
[31] Ivanova VM. Geologic and Stochastic modeling of fracture systems in rocks. PhD thesis, Massachusetts Institute of Technology, 1998.
[32] Hadjigeorgiou J, Lessard JF, Flament F. Characterizing in-situ block size distribution using a stereological model. Can Tunnel 1995:111–21.
[33] Grenon M, Hadjigeorgiou J. A design methodology for rock slopes susceptible to wedge failure using fracture system modeling. Eng Geol 2008;96:78–93.
[34] Grenon M, Hadjigeorgiou J. Fracture-SG. A fracture system generator software package, Version 2.17, 2008.
[35] Dershowitz WS. Personal communication 2007.
[36] Zhang L, Einstein HH. Estimating the intensity of rock discontinuities. Int J Rock Mech Min Sci 2000;37:819–37.
[37] Itasca. Three dimensional particle flow code (PFC3D) V. 4.00. Itasca Consulting Group, Inc.; 2007.
[38] Potyondy D, Cundall PA. A bonded particle model for rock. Int J Rock Mech Min Sci 2004;41:1329–64.
[39] Mas Ivars D, PotyondyD, Pierce M, Cundall P. The smooth-joint contact model. In: Proceedings of the eighth world congress on computational mechanics, Fifth European congress on computational methods in applied sciences and engineering, Paper no. a2735, Venice, Italy, 2008.
[40] Barton N, Bandis S. Some Effects of scale on the shear strength of joints. Int J Rock Mech Min Sci Geomech Abstr 1980;17:69–73.
[41] Itasca, FISH-Lab, Itasca Consulting Group, Inc., 2008.